Arabian Journal for Science and Engineering (2020) 45:1531–1552
https://doi.org/10.1007/s13369-019-04052-w

RESEARCH ARTICLE - ELECTRICAL ENGINEERING

An Alternate Method for Prediction and Analysis of Notch Characteristics in Indoor Power Lines Under Varied Channel Conditions

Rubi Baishya[1] · Banty Tiru[1] · Utpal Sarma[2]

Received: 5 August 2018 / Accepted: 22 July 2019 / Published online: 30 July 2019

Abstract

One of the challenges faced by indoor power line communication systems is the frequency-selective channels that are time varying and dependent on a large number of variabilities. A probable solution is to extract as much determinism as possible through prediction and statistical analysis of the frequency-selective notches. However, such deterministic tools are available only for simple open- and short-circuit branches and not for complex loads and topologies. This paper proposes an alternate method to predict and analyze notches using a minimum of four parameters without evaluating the transfer function. Termed as the load frequency mapping, the method is applicable for any frequency-dependent time-invariant loads and topologies and also capable of performing statistical analysis of random channels. A high decrease in prediction error (99.46–93.63%) is found for all the channels analyzed. Statistical analysis of 26 power line cables using random loads shows that some cables and loads offer more variations in frequency selectivity than others. For capacitive loads, the variation is more for the low-frequency notches and for those modeled as parallel resonant circuits at the frequencies near the resonance. Maximum variation is found for cables with high characteristic impedance with loads having high resonant frequencies and low quality factor and least for inductive loads. The power line therefore has considerable amount of determinism, and this can be incorporated to complement for fading channels or analysis of variability optimized for dual purpose of power delivery and data transfer.

Keywords Power line communication · Transmission line theory · ABCD matrices · Frequency selectivity

Abbreviations

BPLC	Broadband PLC
BW	Bandwidth
CWB	Coherence bandwidth
DMT	Discrete multitone modulation
DB	Derivation box
EMC	Electromagnetic compatibility
FDL	Frequency-dependent load
HAN	Home area network
HAP	House access point
HV	High voltage
IMC	Imaginary characteristics
IA	Input admittance
ISI	Inter symbol interference
IED	Intelligence electronic device
IR	Impulse response
LFC	Load frequency curve
LFM	Load frequency mapping
LPTV	Linear periodic time variant
LV	Low voltage
MTL	Multi-conductor line
MV	Medium voltage
NB-PLC	Narrowband PLC
PL	Power line
PLC	Power line communication
RMS-DS	Root mean square delay spread
SG	Smart grid
SP	Service panel
TEM	Transverse electromagnetic
TF	Transfer function
TL	Transmission line

✉ Banty Tiru
banty_tiru@rediffmail.com

[1] Department of Physics, Gauhati University, Guwahati 14, Assam, India

[2] Department of Instrumentation, USIC, Gauhati University, Guwahati 14, Assam, India

List of Symbols

C	Capacitance/length
L	Inductance/length
Z_0	Characteristics impedance
$Z(\omega)/Z(\omega, t)$	Time-variant load
R	Resistance
ω	Angular frequency
ω_0	Resonant angular frequency
f_0	Resonant frequency
Q	Quality factor
φ	Phase term in time-dependent load
Z_A	Offset impedance
Z_B	Amplitude of variation
$H(f)$	Transfer function
N'	Number of paths
g_i	Complex number
T	Time period
F	Frequency
τ_i	Path delay
$\alpha(f)$	Attenuation coefficient
d_i	Path length
A, B, C, D	ABCD matrices
Z_L	Load impedance
Z_S	Source impedance
f_k^{open}	Open-circuit notch frequency
f_k^{short}	Short-circuit notch frequency
v_p	Phase velocity
l_br	Branch length
Z_in	Input impedance
Z_br	Load in branch
γ	Propagation constant
y	Imaginary load
x	Real component of the load
Y_in	Input admittance
f_1^{open}	First open-circuit notch frequency
w	*Roll-off*
a	Constant
R^2	Regression value
$F_i(y)$	Notch frequency
C1–C26	Cables 1 to 26
$\mathrm{Im}\{Z_\mathrm{br}(f)\}$	Imaginary characteristics of load
Δf	Deviation of frequency
$Y_{IN\text{-}STAR}^N$	IA (*Star*)
Z_total^N	Total impedance at node n
Y_open	IA of open branch
$Y_{IN\text{-}BUS}^N$	IA (*Bus*)
Y_{N-1}	IA of *qp*
y_{N-1}	IA of *qn*
$Y_{\mathrm{open\_}N-1}$	IA of *mq*
$y_{IN\text{-}STAR}^2$	IA of *Star* (2 branches)
$y_{IN\text{-}STAR}^3$	IA of *Star* (3 branches)
$y_{IN\text{-}STAR}^8$	IA of *Star* (8 branches)
$y_{IN\text{-}BUS}^1$	IA of *Bus* (1 branch)
$y_{IN\text{-}BUS}^2$	IA of *Bus* (2 branches)
$y_{IN\text{-}BUS}^6$	IA of *Bus* (6 branches)
L	Inductive load
C	Capacitive load
RLC_1	RLC load (experimental)
RLC_2	RLC load (experimental)
RLC_3	RLC load (experimental)
μ	Mean of notches
σ	Standard deviation of notch
μ_p	Mean of predicted notches
σ_p	Standard deviation of predicted notches
μ_a	Mean of actual notch
σ_a	Standard deviation of actual notch
$\mu_{\Delta f}$	Mean of Δf
$\sigma_{\Delta f}$	Standard deviation of Δf
RLC1	RLC load
RLC2	RLC load
RLC3	RLC load
RLC4	RLC Load

1 Introduction

The use of power lines (PLs) as a communication medium dates back to the early 1900s when the first patents in this line were filed. Commonly known as power line communication (PLC), the technology is quite developed and used by electric utilities round the world for cost-effective value-added services. PLC offers plug and play home/office/industry networking services, automatic remote metering, control services, vehicle to grid communication, applications in smart grid (SG), etc., without any hassle of laying additional cables. PLC can also be used as a component of hybrid networking systems for extended coverage and reliability [1–3]. For successful implementation of such a system, it is required that the individual components are efficiently modeled and systems optimized for maximum efficiency. The PL channel is, however, the most 'horrible' [4] due to time-variant noise [5,6] and frequency-selective transfer functions (TFs) poising channel modeling as the major challenge [7]. If properly addressed, the pervasive and ubiquitous networking facility would provide cost-effective solutions and increased penetration in the mass market.

Frequency selectivity in PLs and specifically deep notches in the transfer function (TF) arises due to reflection in the discontinuities caused by heterogeneous cables and unmatched loads. This leads to small coherence bandwidth (CBW) and large root mean square delay spread (RMS-DS) limiting data rates [8] and mandating complex transmission schemes for mitigation [9–11]. This is more so in low-voltage home area networks (HAN) also known as indoor PL, where the topology is of paramount importance. The situation becomes

worse because the frequency selectivity is time varying due to insertion of time-varying loads or time-invariant ones at unpredictable intervals. As such, an in-depth analysis of the channel is imperative as this helps simplify complex behaviors and generalize the characteristics in an otherwise completely unpredictable scenario. It has also been stated in [12] that 'the PL channel exhibits more determinism than commonly believed and this must be exploited for efficient modem design.' A PL channel that is deterministic or predictable is easier to handle than a completely un-deterministic channel. Channel studies provide two major benefits: firstly, they provide a deeper understanding of the network dynamics making the channel more alluring compared to the 'horrible' description, and secondly, the topological aspects can be incorporated in modems to complement for the fading channels [7]. Determinism in PL channels has led to several methods to mitigate frequency selectivity like precoding schemes for removal of intersymbol interference (ISI) [12], use of adaptive equalizers, in place of linear ones and isolating the resonant modes or notches [13], thus overcoming the drawbacks of noise enhancement. Knowledge of the symmetry nature of the PL regardless of topology reinforces the use of discrete multitone modulation (DMT) as an appropriate modulation technique for PLC [13,14]. The knowledge of the statistical characteristics of the notches also gives a clear understanding of the network dynamics and hence the nature of the information traffic [15] in an ensemble of randomly varying channels . Such studies enable development of standardized channel models with standardized TF wherein coding and modulation can be tested [12] in a simulated environment close to reality.

Indoor PL channels are known to have a large number of variabilities like cable parameters, loads, lengths of cables and topology [16–27]. Loads may be frequency dependent or independent and time variant or invariant arising due to connected appliances to the network [21,25]. The network topologies may be simple to complex like *star* or *bus* connections [28]. The possibility of a large number of variabilities makes the analysis and prediction of frequency selectivity very difficult if not impossible. Much work has been done in this regard, and most are based on modeling the channel or studying the physics of signal propagation through the cables. However, till date, predictability of notches is a big challenge and possible only in a small range of probable loads that are resistive in nature or branches that can be considered as open and short circuits [20,29–31]. These types of loads are, however, only a small range of available classes, and most of the loads are known to be frequency dependent. A complete deterministic study of PL channel should ascertain the predictability of the notches for any change in variability. Till date, no such prediction mechanism is available more so for complex topologies like *star* and *bus* branches. The availability of cables of diverse parameters also motivates to seek general properties of the notches in an ensemble of randomly selected channels and dependency on cable parameters [20]. A method is thus required that can predict and analyze the notches from simple to complex branches and also perform a statistical analysis. This paper aims to present such a technique that is applicable for most of the variabilities found. The scope of this paper is thus twofold: firstly to propose an alternate method of prediction and analysis of notches in indoor PL channels for any change of variables like cables, length and loads, especially for time-invariant and frequency-dependent (FDLs) ones. The method should also be applicable for complex branches like *star* and *bus* branches, and secondly, use the method as a possible mechanism to study the statistical characteristics of channels caused by random loads and generalize the dependency on cable parameters. The proposed method does not necessitate simulation of the TF, but enables notches to be predetermined and analyzed by the knowledge of only 4 parameters necessarily the cable parameters (capacitance per unit length, inductance per unit length), length of the branch and the nature of load at the end of the branch. For any change in the variability, the notches can still be determined with minimum computational cost or simply by visual mechanism. Such knowledge apriori in a network can be incorporated in modem designs to handle unpredictability with lesser complexity. Though notches are characterized by the attenuation which is affected by the nature of the loads [29], the position of the branches [29] in the main circuit and also the number of branches [32], these are left as a future work. The time-variant FDLs are also not analyzed in this paper.

This paper starts with a brief introduction of PLC in different stages of the PL grid both outdoor and indoor. The necessity of notch prediction and analysis, especially in the case of indoor PL section, is then presented. A technique termed as load frequency mapping (LFM) is developed using results from a simple analysis of the characteristics of notches. This is then verified in simulated and experimental environments and applied to perform a statistical analysis. The paper is sectioned as follows: In Sect. 2, a brief overview of the PL grid and PLC in general is presented. This is followed by a comprehensive literature review on the variability in indoor PL channels, modeling techniques and limitations in regard to prediction in Sect. 3. Section 4 analyzes the notches characteristics in detail using the input admittance (IA) of the branches. This analysis is used to develop and present the LFM technique. In Sect. 5, the applicability of the LFM technique is verified under various simulated and practical channel conditions. In Sect. 6, the LFM is used to perform a statistical analysis of randomly selected loads and generalized for different types of loads and the characteristic impedance of the cables. Section 7 discusses and summarizes the results and presents the importance of the work in comparison with other available methods. This is followed

by a conclusion of the work with probable applications of the technique.

2 The Power Line Grid and Power Line Communication

The PL grid consists of three sections: generation, transport and distribution and comprising three stages, namely the high-voltage (HV) lines (110–380 kV), medium-voltage (MV) lines (10–30 kV) and low-voltage (LV) lines (100–400V). In the MV networks, there are three topologies to deliver electricity like radial, ring or networked. The LV lines directly lead to the customer's premises using various topologies like *star*, T-off or direct connection. The electricity grid enters the premises using the house access point (HAP) followed by an electricity meter and a distribution box. Out of these, the HV is rarely used for PLC. The MV has been under trial for narrowband PLC (NB-PLC) in the frequency band < 500 kHz for control applications and intelligent electronic devices (IED) such as reclosers, capacitor banks and phasor measurement units in SG applications [33]. The broadband signals are also injected at the MV or at the LV stages [34,35] of the grid to carry forward to indoor PL through the HAP. The PLC to the HAP is called the access PLC. The LV indoor PL can be used for in-house or control applications using both NB-PLC and Broadband PLC (BPLC). BPLC uses a wide band of (1–30) MHz for high-speed data communication. In the MV, such variability like cabling methods (underground, overhead or bare overhead), ground impedance, injection points of PLC signal, modeling and impact of transformers, loading conditions, elements of voltage regulation and compensation (shunt capacitors, series capacitors, shunt reactors), etc., becomes important parameters [36–40]. For example, the shunt capacitors used in radial distribution networks are supposed to be placed and sized for optimizing and minimizing the effects using different algorithms like flower pollination algorithms, etc. [41,42]. This geometry must be taken into consideration in a practical PLC model that incorporates every variability of a practical PL channel scenario. In indoor PLC, the topology of electrical distribution, loads used and cables are the determining factors of frequency selectivity. These must be studied in detail for any sort of determinism. In our work, our focus is mainly on the indoor PL to provide a possible method of prediction and analysis.

3 Literature Review on Variability of Indoor Power Line Channels, Modeling and Analyzing Methods and Limitations in Regard to Prediction and Analysis

In this section, a literature review on the nature of indoor PL channels specifically the variability, the modeling methods available to analyze the channels and limitations related to predictability and analysis is done.

3.1 Variability in Power Line Channels

PL channels are unlike other wired systems, and the characteristics depend on a large number of variables. The variability that makes the channel so unique compared to other wired systems is given as follows:

3.1.1 Cable Parameters

The cable parameters of PLs vary in a wide range. Table 1 gives some of the cable parameters obtained in different papers [16–24]; Cable C8 is used in this work for simulation and experimental verification. The cable has inductance per unit length, capacitance per unit length, conductance per unit length and characteristic impedance of $L = 0.69\ \mu$H/m, $C = 38$ pF/m, $G = 0.018\ \mu$ mho/m and $Z_0 = 134.7\ \Omega$, respectively. As seen from the table, the Z_0 varies in a wide range of 268.3 Ω to 7.2 Ω (not limited to) resulting in implications in the frequency selectivity that is further analyzed.

3.1.2 Network Topology

The distribution topologies of indoor PL are of varied types. An indoor PL distribution may be multi-meter system in multi-flat buildings with riser; single meter in multi-flat buildings; single meter with distribution in a house etc. In [17], the distribution inside the house has a derivation box (DB) where power may be led to the service panels (SPs) through *star*, *bus* or *star* along the perimeter configurations. The *star* topology satisfies the minimum distance criteria between the DB and the SP, the *bus* topology has conductors placed along the perimeter, and the *star* along perimeter configuration is actually *star* topology connected through the perimeter [27]. A transmitter and receiver of PLC device may be placed anywhere along the distribution network, and the network in between may be very complex. However, papers have simplified the network for the sake of analysis in a number of ways. For example, in [25], the main path between the transmitter and the receiver consists of stubs or 'bridged taps,' and in [21], the main line consists of branches in *bus* configuration that may also be *star* in nature . In [26], the branches may themselves be of *bus* types. In this paper, we simplify the path between the transmitter (X) and receiver (Y) as consisting of stubs or branches in three topologies such as a simple branch, a branch ending in *star* topology and a branch of *bus* type as shown in Fig. 1. A *star* branch has a large number of branches at the node, but in *bus*, the branches emanate in a serial way. Large topology networks decrease the CBW of the channels [21] considerably.

Table 1 Cable parameters of different power line cables found in papers together with the *roll-off* constant *w*

Cable [References]	L (μH/m)	C (pF/m)	$Z_0(\Omega)$	LC (10^{-18})	R^2	w (10^{-3})
C1 [17]	1.08	15	268.32	16.2	0.9942	1.77
C2 [17]	0.96	17.5	234.21	16.8	0.9956	2.03
C3 [17]	0.87	20	208.56	17.4	0.9969	2.28
C4 [18]	5.9	167	187.96	98.5	0.8877	2.53
C5 [17]	0.78	25	176.63	19.5	0.9982	2.7
C6 [19]	0.54	26	144.11	14	0.9988	3.3
C7 [17]	0.68	33	143.54	22.4	0.9988	3.32
C8 [20]	0.69	38	134.75	26.2	0.9988	3.53
C9 [16]	0.65	40.3	127	26.2	0.9989	3.75
C10 [19]	0.51	33	124.31	16.8	0.9988	3.83
C11 [21]	1	80	111.8	80	0.9985	4.26
C12 [51]	0.44	61.73	84.42	27.2	0.9972	5.64
C13 [19]	0.48	77	78.95	37	0.968	6.03
C14 [19]	0.31	56.8	73.87	17.608	0.9963	6.45
C15 [22]	0.3	57.5	72.23	17.25	0.9962	6.59
C16 [23]	0.25	138	42.56	34.5	0.9918	11.2
C17 [23]	0.17	191	29.83	32.47	0.9887	16
C18 [23]	0.14	190	27.14	26.6	0.9879	17.5
C19 [23]	0.12	237	22.5	28.44	0.9863	21.2
C20 [23]	0.11	247	21.1	27.17	0.9845	22.6
C21 [24]	0.04	156.5	15.98	6.26	0.9841	29.8
C22 [23]	0.083	313	16.28	25.979	0.9839	29.2
C23 [23]	0.089	372	15.46	33.108	0.9812	30.8
C24 [23]	0.082	371	14.86	30.422	0.9833	32
C25 [23]	0.039	656	7.71	25.584	0.9796	61.8
C26 [23]	0.04	756	7.27	30.24	0.9793	65.5

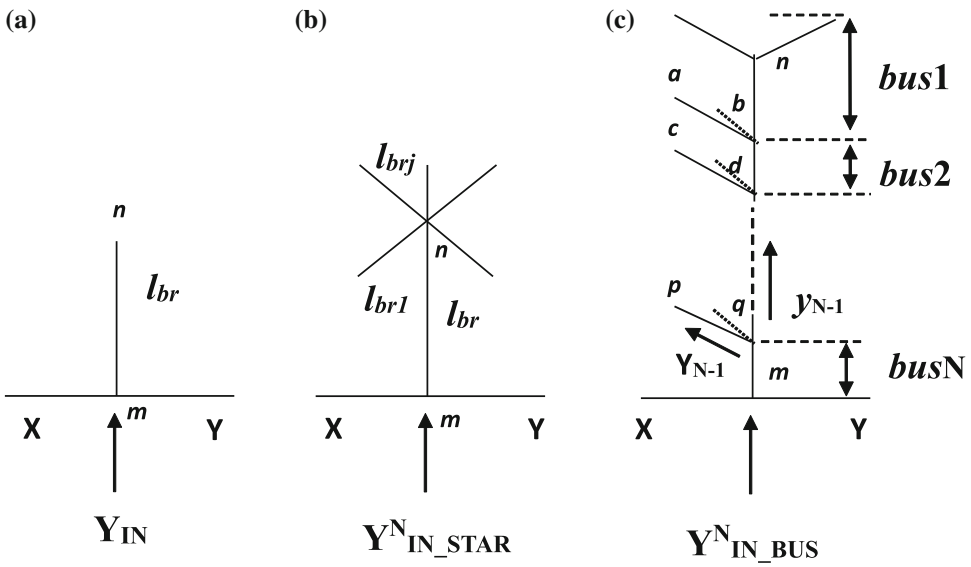

Fig. 1 Different types of branches *mn* encountered in the communication path XY: **a** simple branch, **b** *star* branch and **c** *bus* branch in a transmission path XY

3.1.3 Loads in Power Line Channels

Branches in PLs are loaded with varied types of loads that may be frequency independent or dependent. These loads arise due to equipments connected to the PL. In [21,25], the loads are classified into three groups: (i) constant impedances (ii) time-invariant FDLs and (iii) time-varying FDLs. Loads in category (i), are resistive in nature, with values like 5, 50,

150, 1000, 108 Ω representing low, RF standard, nearly equal to the Z_0, high and infinite impedances, respectively. Very few loads have this nature. The loads in group (ii) are in the form of parallel RLC resonant circuits, whose impedance is given by (1)

$$Z(\omega) = \frac{R}{1 + jQ\left(\frac{\omega}{\omega_0} - \frac{\omega_0}{\omega}\right)} \tag{1}$$

consisting of R, the resistance at resonance, ω_0, the resonant angular frequency ($\omega_0 = 2\pi f_0$, f_0 being the resonant frequency), ω, the angular frequency and Q, the quality factor. The parameters of RLC loads ranged $R \in \{200, 1800\}$ Ω, $f_0 \in \{2, 28\}$ MHz, and $Q \in \{5, 25\}$ [23]. The load in the group (iii) is dependent on the AC mains signal and modeled as (2)

$$Z(\omega, t) = Z_A(\omega) + Z_B(\omega)\left|\sin\left(\frac{2\pi}{T}t + \varphi\right)\right|; 0 \le t \le T \tag{2}$$

This group may either have two states of impedances or with smoother variations having a periodicity of $F = 1/T = 50$ Hz. It has a rectified sinusoid that is synchronized with the AC mains. The three parameters Z_A, Z_B and φ are the offset impedance, the amplitude of the variation and a phase term that references the instantaneous impedance with the mains signal. In [43], the loads are modeled as of three classes: A, B and C. Class A devices have monotonically increasing magnitude of the impedance, equipped by an X capacitor at the feeding point, and shows the same characteristics regardless of their operating states. Class B devices show damping peaks and nulls and subdivided into Class B-1 (inductive) and Class B-2 (capacitive) depending on the behavior at low frequencies. Class C devices are time-varying loads that show two states of impedances in the cycle of the AC mains. The Class C loads and those modeled by (2) give rise to linear periodic time-variant (LPTV) nature of the PL [25]. Extensive measurement in PLs [21] shows that most of the loads can be modeled as resonant-shaped impedances given by (2), and those with LPTV also can be modeled so for a large fraction of time [44]. Few devices show the time-varying nature, significant only in frequencies below 2 MHz [45] being suppressed by the electromagnetic interference filters used in power supplies. In [19,30], capacitive loads and inductive loads are also included, respectively. The capacitive loads mainly occur because of electromagnetic compatibility (EMC) capacitors, the maximum value of which is 0.49 μF and most common is 0.1 μF [19]. The inductive loads are in the mH range.

The presence of a large number of variabilities in PL channels makes the channel very heterogeneous causing multipath reception and hence to an extremely frequency-selective channels requiring efficient analyzing tools.

3.2 Modeling Method of Indoor PL Channels for In-Depth Analysis of Frequency Selectivity and Limitations in Regard to Prediction

As discussed in the preceding section, the TF of the PLs is dependent on several variables, making prediction a non-trivial task. However, an attempt to correlate the observed with the physical origins through modeling simplifies the problem. Modeling provides a way to analyze the observed minutely and also gives an idea of how the channel will act in different network conditions. This section describes in brief some of the modeling methods used to model and analyze the frequency selectivity.

3.2.1 Time Domain Top-Down Model: The Multipath Model

In the top-down approach [12], the frequency selectivity of PLs arises due to reflections at the myriad discontinuities constituting the network. Multipath reception with different propagation delays and phase causes frequency-selective fading in the channel. The time domain approach is also called the echo model and involves expressing the TF as a function of four parameters: g_i, a complex number that depends on topology; $\alpha(f)$, the attenuation coefficient; τ_i, delay associated with ith path, d_i , the path lengths and N', the number of nonnegligible paths. The TF in the echo model can be written as (3) [12]

$$H(f) = \sum_{i=1}^{N'} g_i e^{-j2\pi f \tau_i} e^{-\alpha(f) d_i} \tag{3}$$

The major drawback of this method is that the parameters can be estimated only after the measurement of the actual TF and the computational cost of estimating the delay, phase and amplitude of each path is very high. Due to lack of the knowledge of the port impedances, it is difficult to generate all the different paths individually and hence analyze the network. Prediction of notches and dependency on variability cannot be done, but [14] extends the method to statistical analysis.

3.2.2 Frequency Domain Bottom-Up Model: The Deterministic Method

The frequency domain bottom-up approach [12] uses the transmission line (TL) model (two or three wires, the latter termed as multi-conductor (MTL) to predict the TF accurately. The TL model assumes the signal to be propagated in a PL as transverse electromagnetic (TEM) wave and help in visualizing the effect of all the reflections at the disconti-

nuities enabling the salient features to be extracted. Unlike the multipath model, this method is a deterministic approach which requires everything about the channel to be known *aprior*; for example, the topology, the type of cables used, the loads in the branches, etc. and is the price that cannot be avoided. Matrices like the transmission matrices, ABCD matrices and scattering matrices are used to evaluate the TF [29,32]. The MTL approach takes into consideration the presence of the third grounding conductor, grounding practices and the common mode currents related to EMC as well. In the case of ABCD matrices, the PL network is taken as cascaded sections and the TF written in terms of the overall matrices given by (4) [29,32]. Here, Z_S and Z_L are the source and load impedance, respectively.

$$H(f) = \frac{Z_L}{AZ_L + B + CZ_SZ_L + DZ_S} \tag{4}$$

This method has been used extensively to study the characteristics of notches [28,29,46] and offers a simple method of analyzing. It has been found that the number of notches increases with the length of the branches showing a periodic nature [29,32] . The attenuation is determined by the loads at the terminations and exaggerated by multiple ones at the same frequency [32]. Resistive loads cause the notches to be at open and short circuits depending on the values, but complex loads, especially the FDLs, shift the notches from these positions [29]. Analysis of frequency selectivity for different loads, cables and statistical analysis can be done using this method. The problem with this method is that determinism is possible only after simulating the TF, but there is no way of prediction of the notches. For any change in variability, the TF has to be simulated all over again to have an idea of the frequency selectivity.

3.2.3 Statistical Models

The statistical models take into consideration the stochastic description of PL channels owing to the large variability of link topologies and wiring practices that affects the performance of the PLC devices [47–49]. The statistical implications usually come from measurements. It has been found that the RMS-DS are log normally distributed and channels that induce severe multipath are also found to have high attenuation [47]. The characteristics of the notches like the peak and width of the notch, heights and numbers are well described by Rayleigh, triangular and Gaussian distributions [48]. In [49], authors have analyzed that for all types of loads, the impedance parameters follow a Lognormal-3P distribution. The statistical models usually do not rely on the underlying physical structure of PL, and as such, the information they provide is limited to the description of the TF only. The limitations of the statistical method are that the correlation between the physical structures of the PL is lacking. This prevents any sort of prediction or dependency on any variability. Statistical analysis therefore cannot be done.

3.2.4 RLC Resonant Circuit

In this modeling method, the PL branches are taken either as parallel [50] or series [31] RLC resonant circuits attached to the main line [31,50]. For a parallel RLC circuit, the input impedance of the branch is minimum at resonance, which gives rise to notches.. This concept, however, is applicable for a less number of branches and the accuracy decreases for a large number of branches [50]. Only open or short circuits are analyzed using this method, and the concept cannot be used for any other types of loads. In [31], the branches are considered as a number of series resonant circuits, with open and short circuits represented as quarter and half wavelength TL lines. Here too the deterministic model covers only open- and short-circuit branches. The RLC methods are thus deterministic only for open and short circuits, but not for any change in variability or for performing a statistical analysis.

3.2.5 IIR Filter Approach

In this method, the elements of the channel like line discontinuities, branches, general loads and *star* junctions are modeled as IIR filter elements [51]. The overall TF is obtained by concatenating the TF of the individual filters. The problem with this method is that it is very complex because every component is represented in the form of filters. The general load is taken as frequency independent, and FDLs necessitate the computations to be more complex. Stochastic description of the channel is also not done here.

3.2.6 Voltage Ratio Method

This method simplifies complex branches in the propagation path by identifying the shortest distance between the transmitter and receiver also called the backbone. The complex branches are then collapsed back onto the backbone using the impedance carry back method, and the TF is expressed as a ratio of the voltages at the input to output ports [27]. Statistical analysis is possible with this method [15]; however, prediction of notches is not done.

3.2.7 Transmission and Reflection Factors

Here, the loads, interconnections and distances are visualized in terms of transmission and reflection factors [52]. However, this model is verified for resistive loads only. Statistical analysis of the notches is also not done.

3.2.8 Other Deterministic Models

In addition to methods described above, some other expressions are available that arise from analysis [30] or the physics of signal propagation [29,31] expressed as generalized expressions [30], the phase velocity [31], the wavelength of the signal [29] or derived from the phase constant , of the cables [20]. In regard to phase velocity, the open- and short-circuit notches are given by (5) and (6), respectively.

$$f_k^{\text{open}} = \frac{v_p}{4l_{\text{br}}}\left(2k'+1\right) \tag{5}$$

$$f_k^{\text{short}} = \frac{v_p}{4l_{\text{br}}}\left(2k'\right) \tag{6}$$

where l_{br} is the length of the branch, v_p is the phase velocity and k'=1,2..... In [29], the open- and short-circuit frequencies are those for which the path difference caused by the cables is odd multiple of $\lambda/2$ and multiples of λ, respectively, where λ is the wavelength of the signal. Considering the phase constant in the cables, the open- and short-circuit notches can also be expressed as [20] (7) and (8), respectively

$$f_k^{\text{open}} = \frac{2k+1}{4l_{\text{br}}\sqrt{LC}} \tag{7}$$

$$f_k^{\text{short}} = \frac{k}{2l_{\text{br}}\sqrt{LC}} \tag{8}$$

Here, $k = 0, 1, 2\ldots$.The limitations with these deterministic models are that these are available only for open- and short-circuit branches but not for complex topologies and varied loaded conditions, especially the FDLs [29]. For shorter branches, the notches are easier to predict and occur at positions where the impedance of the loads is minimum [16], but for longer branches become in cognizable.

Though lots of work is done in this area, a method or technique that can predict notches for any change in variability is still lacking. A comparison of the available prediction and modeling method and limitations are given in Table 2. As seen from the table, none of the listed methods enable deterministic prediction of notches and analysis on the dependencies of the network. The only method that fulfills these criteria is the frequency domain deterministic method that, however, necessitates the evaluation of the entire TF for any change in variability. In this paper, an alternate method is presented to overcome the limitations of the available methods. The technique is a deterministic method and enables analysis of any types of FDLs without the evaluation of TF by a simple method. The method is developed using the simple TL theory and verified using the frequency domain deterministic method specifically the ABCD matrices described in Sect. 3.2.2.

4 Proposed Load Frequency Mapping Technique for Prediction and Analysis of Notches

To develop the LFM technique, an analysis of the notches in a one branch PL channels is initially done. This is performed using the input admittance (IA) of a simple branch loaded with real and constant imaginary loads. The loci of the notches show distinctive features that are fitted using a curve termed as the load frequency curve (LFC). The LFC enables prediction of notches for any type of cables, branch lengths and FDLs and described in the succeeding sections. In all the simulation and verification (simulation or experimental) experiments, cable C8 is used unless stated.

4.1 Preliminary Analysis of Notches Using Input Admittance of Branches

The notches in the TF of a PL channel are determined by the branched circuits in the propagation path. The notches occur at frequencies at which the input impedance of the branches is minimal or the IA is maximal so as to provide easy paths for the signal. As such, it is enough to analyze the IA to determine the characteristics of the notches. From the TL theory, for a cable of length l_{br} and loaded with load Z_{br} , the input impedance and IA are given by (9) and (10), respectively [28]

$$Z_{\text{in}} = Z_0\frac{Z_{\text{br}} + Z_0\tanh(\gamma l_{\text{br}})}{Z_0 + Z_{\text{br}}\tanh(\gamma l_{\text{br}})} \tag{9}$$

$$Y_{\text{in}} = \frac{1}{Z_0}\frac{Z_0 + Z_{\text{br}}\tanh(\gamma l_{\text{br}})}{Z_{\text{br}} + Z_0\tanh(\gamma l_{\text{br}})} \tag{10}$$

where Z_0 and γ are the characteristic impedance and the propagation constant of the cable, respectively. For analysis, real and imaginary loads are inserted in the terminations of the simple branch shown in Fig. 1a. The frequencies of the maxima of the IA are found out which give the frequencies of the notches. From simulations using (10), it can be concluded that

1 For constant resistive loads Z_{br}= x, the notches are either at f_k^{open} or f_k^{short} according to the value which is greater or less than Z_0. These frequencies are given by (7) and (8), respectively. Figure 2a shows the locus of the position of the notches as x is increased from 0 to 1000 Ω. For a branch length of l_{br} = 2.55m, f_k^{open} =19.2 MHz, 57.4 MHz.... and f_k^{short} =38.3 MHz, 76.5 MHz..... and flips into position at x=134.7 Ω.
2 Figure 2b shows the locus of the position of notches for loads with only a constant imaginary component such as $Z_{\text{br}} = jy$ when the value of y is changed from +2000 to − 2000. The notches are at f_k^{short} or f_k^{open} for very small

Table 2 Comparison of the proposed method for notch prediction and analysis with available methods for PL channels

Models used for analyzing the frequency selectivity of PL channels	Method used	General limitations of method	Notch prediction	Limitation regarding		
				Dependency on cable parameters	Dependency on loads	Statistical inferences
Time domain echo	Multipath reflection with different propagation and phase delay results in frequency selectivity	High computational cost, parameters are obtained only after the measurement of the actual TF	X	X	X	✓
Frequency domain deterministic	Use transmission, ABCD or scattering matrices to visualize reflections at discontinuity and estimate frequency selectivity	Every component should be known apriori	✓ (Only after evaluation of the TF)	✓ (Only after the evaluation of TF)	✓ (Only after evaluation of the TF)	✓ (Only after extensive simulations)
Statistical models	Stochastic description of PL channels owing to the large variability	Limited to description of TF only. Cannot correlate with the physical parameters of the channel	X	X	X	X
Parallel RLC resonance circuits	Branches are modeled as parallel RLC circuits. The resonance frequencies are the frequency of notches	Applicable for a less number of branches only and only open and short circuits	Only for resistive loads	X	X	X
Series RLC Circuits	Branches are modeled as series RLC circuits. Open and short circuits represented as quarter and half wave TL lines	Applicable for open and short circuits only	Only open and short circuits	X	X	X
Channels as concatenated IIR filters	Components of the network are considered as IIR filters	Validated for frequency-independent loads and stochastic analysis not done	X	X	X	X
Voltage Ratio Method	Simplify complex network by impedance carry back method and evaluate TF in the form of voltage ratio	The reflection coefficient needs to be evaluated every time	X	X	X	✓
Transmission and reflection factors	Transmission and reflection factors at every interconnection, length and load determine the frequency selectivity	Verified for only resistive loads only	Only resistive loads	X	X	X
Phase velocity or wavelength of signal propagation.	Physics of signal propagation	Only for open and short circuits	Only open and short circuits	Only for open and short circuits	Only for open and short circuits	X
Proposed LFM method	Modeling the variation in notch frequency for constant imaginary loads and estimating the notch frequency using LFM technique	Not analyzed for time-variant FDLs	✓ (Only 4 parameters are necessary)	✓ (only 4 parameters are necessary)	✓ (Only 4 parameters are necessary)	✓ (Only 4 parameters are necessary)

N.B: X Not available; ✓ available/possible

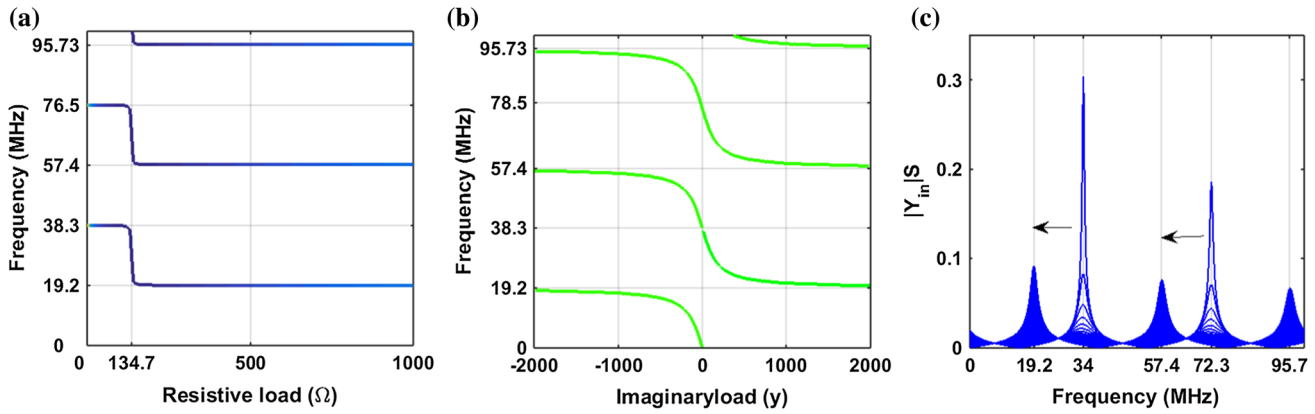

Fig. 2 **a** Locus of the frequency notches for constant loads of the type $Z_{\text{br}} = x$. **b** Locus of the notches for constant imaginary loads such as $Z_{\text{br}} = jy$. **c** Magnitude of the input admittance $|Y_{\text{in}}|$ of a simple branch in Seimen(S) for complex loads of the type $(x + 50j)$ when x is varied from 0 to 5000 Ω, the arrows showing the notches shifting to the open-circuit positions for large values

or large values of y , respectively, but shifted for medium ones. The locus of the shift follows deterministic pattern and depends on the length of the cable and the cable parameters L and C.

3 For loads that are complex in nature, such as $Z_{\text{br}} = x + jy$, the positions of the notches are determined by y for small values of x. Figure 2c shows the magnitude of the IA or $|Y_{\text{in}}|$ in Siemens (S) of a simple branch loaded with complex load $Z_{\text{br}} = x + j50$. The value of x is changed from 0 to 5000 Ω to observe the effect. For small values of x, the imaginary part causes the notches to be at 34 MHz, 72.3 MHz, etc. But as the value of x increases, the notch is shifted to the open-circuit position. This shift is shown by the arrow in the figure. The real component of the load x also determines the height of the peaks rendering it minimum for moderate values (between 100 and 500 Ω in this case).

From this analysis, it is found that the imaginary component of the load shifts the frequency of the notches and the determining factor for any load conditions. Large values of the real components only cause the notch to be shifted to the open-circuit position.

4.2 Fitting the Locus of the Notches Using the Load Frequency Curve (LFC)

From Fig. 2b, it is seen that the locus of the first notch has a value of zero at $y = 0$ and increases to 19.2 MHz at large negative values of y. These are just replicated for a higher number of notches. These are fitted with suitable curves to develop the LFM technique. The locus of the first notch can be empirically fitted using the function $F_1(y)$ as given by (11). The frequencies F_1 on the curve are the notch frequencies that are satisfied for specific values of y. Here, f_1^{open} is the frequency of the first open-circuit notch evaluated using $k = 0$ in (7) and w is a constant that represents the change of $F_1(y)$ or *roll-off* at small values of y. Analyzing the locus of the notches for a large number of cables given in Table 1, it is found that greater is the Z_0 of the cables, the smaller is the w and vice versa. As such, w can be modeled as (12) where the constant 'a' is found out by maximizing the R^2 of the fitting. The consecutive loci can be found by the recurrence relation $F_i(y)$ as given by (13) . Alternately F_2, F_3 …with $i = 2, 3$ …are the frequencies of the second and third notch satisfied by the specific value of y. These fitting curves altogether are called the load frequency curve (LFC). Figure 3a shows the fitting of the LFC with the locus of the notches for different values of 'a.' It is found that w fits up to a high value of the $R^2 = 0.9989$ when the value of the constant $a = 2.1$. For other values of a, the R^2 is smaller than this. This is shown in Fig. 3b.

$$F_1(y) = -f_1^{\text{open}} \tanh(wy) \tag{11}$$

$$w = \frac{1}{a\sqrt{L/C}} \approx \frac{1}{aZ_0} \tag{12}$$

$$F_i(y) = 2f_1^{\text{open}} + F_{i-1}(y) \tag{13}$$

From Table 1, it is seen that an increase in the Z_0 from 7.2 Ω to 268.3 Ω decreases the value of w from 0.0655 to 0.00177. To verify the generalization of this model for different cables (C8, C9 and C11 of Table 1), the contour plot of the IA with a single branch loaded with different constant imaginary loads ranging from very small to large values is found out using (9). This is shown in Fig. 4. The LFC model is evaluated using (11)–(13) for the specific L and C and is then superimposed on the contour plot. It is found that the LFC correctly models the shift of the IA maxima or the position of the notches for the cables tested. Considering all the cables in Table 1, the average R^2 of the fitting is given by 0.9866. The LFC correlates all the variables like the length of the

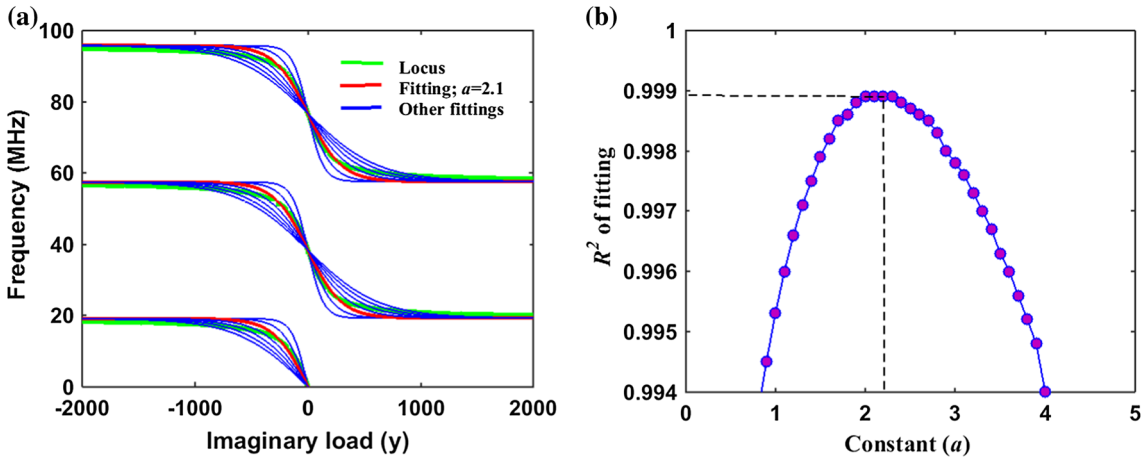

Fig. 3 **a** Fitting of the locus of the notches with the LFC for different constants 'a.' **b** Variation of R^2 of the fitting curves for various values of 'a', showing maximum value for $a = 2.1$

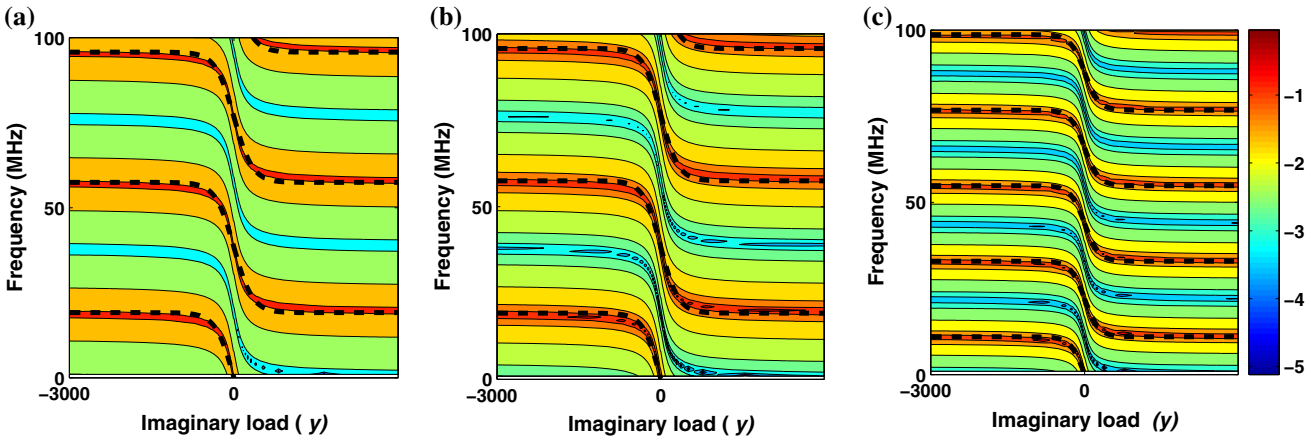

Fig. 4 Contour plot showing the variation in the magnitude of the input admittance of a power line section with one branch loaded with different constant imaginary loads. Superimposed is the LFC (dotted) from the model. The cables are given by **a** C8, **b** C9, **c** C11

branches and the cable parameters (L and C) and can be evaluated using only these three parameters. In the next section, the LFC is used to predict the notch for any type of FDLs.

4.3 The Load Frequency Mapping Technique

From the analysis in the preceding sections, it is seen that the locus of the notches follows a deterministic pattern given by the LFC. Also, from Fig. 2b, it is seen that the notch at a particular frequency occurs for a particular value of the imaginary load. For FDLs, as the imaginary characteristics (IMC) or $\mathrm{Im}\{Z_{\mathrm{br}}(f)\}$ of the loads vary with frequency, notches will occur only if the value of the IMC at a particular frequency is equal to the value of the imaginary load at the same frequency as given by the LFC. Hence, finding out the frequency where these two are simultaneously satisfied can enable the prediction of notches. The block diagram or algorithm for the LFM technique for notch prediction is shown in Fig. 5. In the first step, using L, C and l_{br} as the input parameter, the first open-circuit notch frequency f_1^{open} and the *roll-off* constant 'w' are found out for the cable of interest. Next, the LFCs for this cable, for example, $F_1(y)$, $F_2(y)$, etc., are estimated using the fitting models (11)–(13). In the third step, the frequencies of simultaneous satisfaction of the LFC and IMC are found out. The frequencies can also be obtained by superimposing the IMC with the LFC. The frequency of simultaneous compliance gives the frequency of the notches. Thus, if f_1 and f_2 are the frequencies for the first and second notch, then (14) and (15) are satisfied.

$$\mathrm{Im}\{Z_{\mathrm{br}}(f)\}|_{f=f_1} = y|_{F_1=f_1} \tag{14}$$

$$\mathrm{Im}\{Z_{\mathrm{br}}(f)\}|_{f=f_2} = y|_{F_2=f_2} \tag{15}$$

Using such equation, the higher frequency is also estimated. If the characteristics of the IMC are such that the LFC is not intersected at any frequencies, then no notches occur

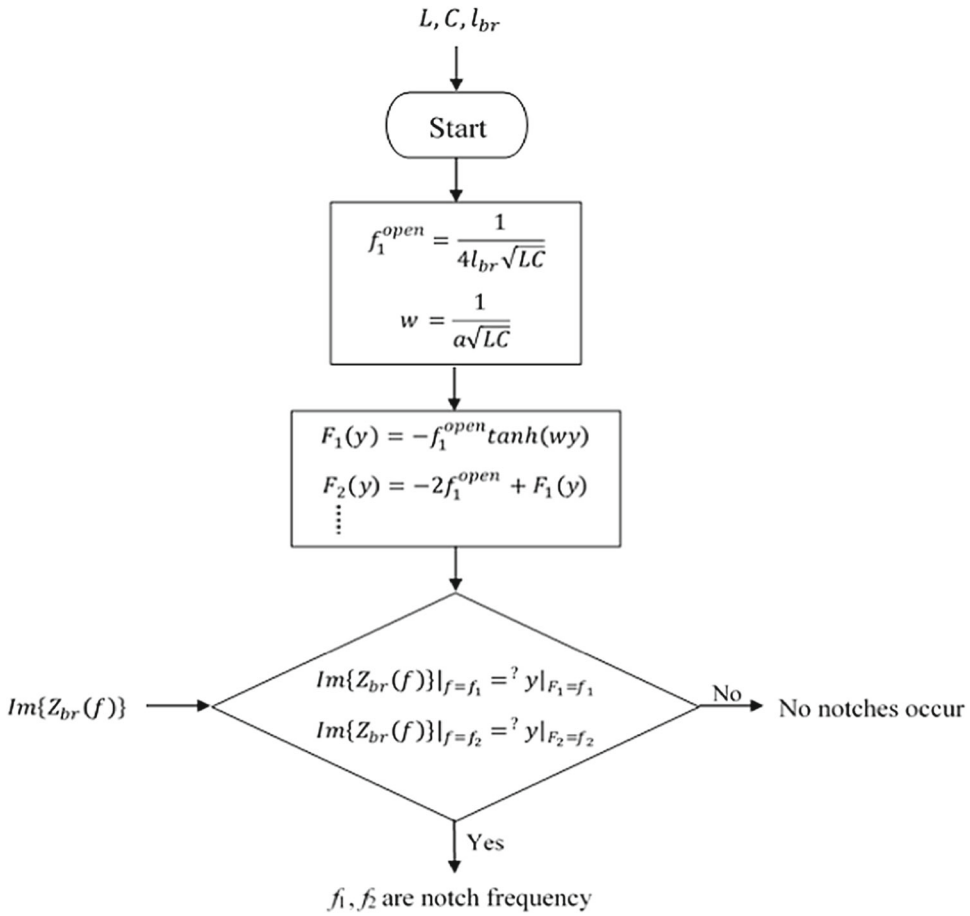

Fig. 5 Block diagram of the LFM technique for prediction and analysis of notches in indoor PL channels

in the given bandwidth (BW) of observation. The LFM can thus be taken as a mapping from the load characteristics to the notch frequency through the LFC. The LFC thus does away with the evaluation of the TF or IA for analyzing the notches. In the next section, the procedure is verified for different channel variabilities described in Sect. 3.2.

5 Verification of the LFM Procedure

In this section, the LFM procedure is verified by simulating test channels constituted of time-invariant FDLs, complex topologies and random loads. The procedure is also tested experimentally.

5.1 Simulated Test Channels

For simulated cases, three classes of network conditions are considered: firstly, the time-invariant FDLs in a simple branch, secondly, branches having complex topologies and thirdly, random FDLs in a simple branch. The first class is broadly divided into (i) capacitive loads (ii) inductive loads and (iii) resonant RLC loads. For the second class, two cases are considered: (iv) *star* topology with a different number of branches and (v) *bus* topology with a different number of *bus* components. For the third class, the FDLs of the first class are chosen randomly and the applicability analyzed in terms of statistical parameters. For each test channel, the frequency of the notch is estimated from the LFM and also from (4) or (9) and termed as 'predicted' and 'actual', respectively. The difference between these two gives the deviation of frequency Δf and can be taken as a measure of the efficiency of the LFM method. The smaller is the Δf, the greater is the accuracy of prediction or the lesser is the error.

5.1.1 Time-Invariant FDLs in a Simple Branch

For (i)–(iii), the loads are inserted on a simple branch of length $l_{\text{br}} = 2.55$ m. Figure 6 shows the TFs and the LFMs for capacitive (100 pF), inductive (0.1 mH) and RLC loads whose (f_0, Q, R) are given by (22 MHz, 5, 200 Ω). It is seen that the IMC intersects the LFC at 3, 3 and 2 points, respectively, and hence predicts the same number of notches. This is also confirmed by the TF. The exact positions of the notches (both actual and predicted) are noted in the figures. The Δf of the notches for the three loads are given by (300 kHz,

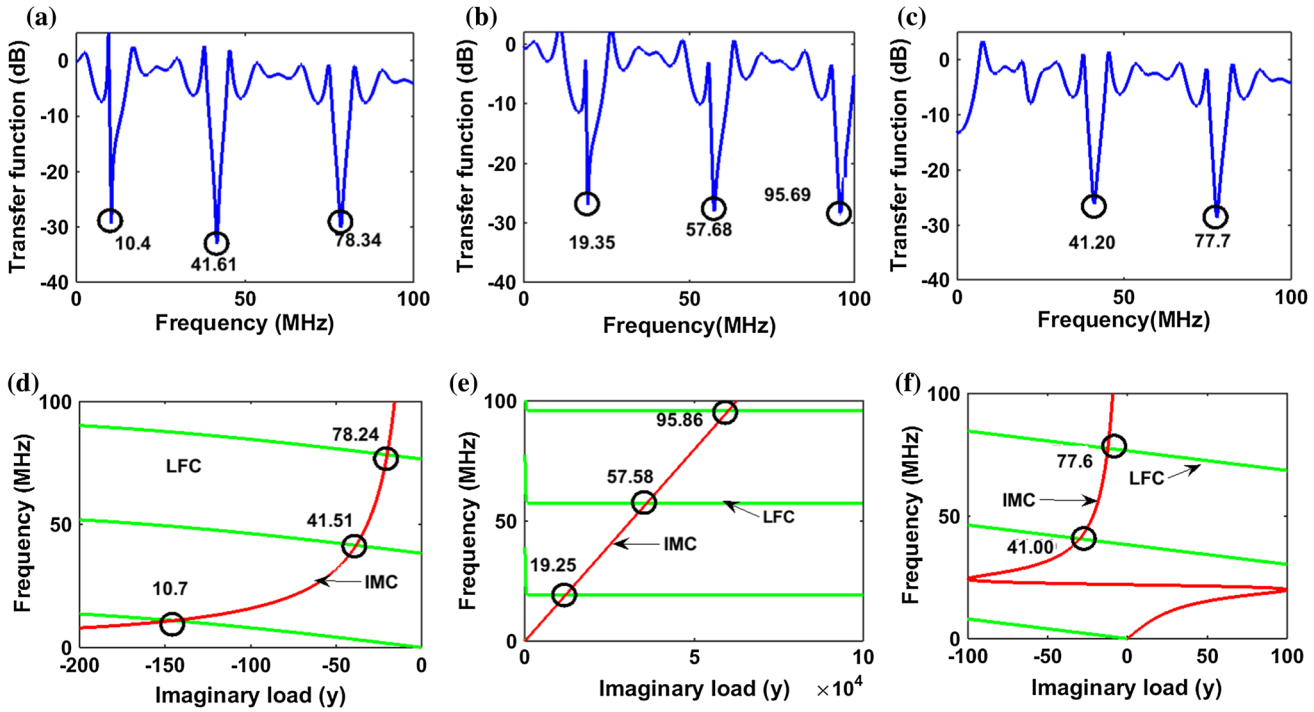

Fig. 6 Verification of the LFM procedure using FDLs. The magnitude of the transfer function of a power line section with one branch loaded with **a** capacitive load, **b** inductive load, **c** RLC load. The LFM is given in **d**, **e** and **f**, respectively. The actual and the predicted notch frequencies (in MHz) are noted in the figures

100 kHz, 100 kHz), (100 kHz, 100 kHz, 170 kHz) and (200 kHz, 100 kHz), respectively.

Implications The LFM technique can be applied for prediction of notches for FDLs without evaluation of the TF within a limit of error.

5.1.2 *Star* Topology

In the case of *star* topology, the number of branches in the *star* node n (Fig. 1b) is increased from 2, 3 and 8 numbers which are all considered as open circuits. The 8 numbers of branches are of random lengths. The positions of the notches are evaluated using the IA of the main branch (mn) at node m. As noted earlier the IA peaks, denote the frequency of the notches. For N numbers of *star* branches, the IA is given by (16) [28]

$$Y^N_{IN\text{-}STAR} = \frac{1 + Z^N_{\text{total}} Y_{\text{open}}}{Z^N{}_{\text{total}} + Z_0^2 Y_{\text{open}}} \tag{16}$$

where Y_{open} is the IA at the node m if mn were open and Z^N_{total} is the total impedance offered by the *star* at the node n. Figure 7 plots the IA, namely $|Y^2_{IN\text{-}STAR}|$, $|Y^3_{IN\text{-}STAR}|$and $|Y^8_{IN\text{-}STAR}|$ for the cases. A total of 5, 10 and 15 peaks occur, respectively, although for some the heights are too small to detect. The frequency of the peaks is taken as 'actual' values. As the number of *star* branches is increased, the notch near the short-circuit frequency becomes predominant. Next, the IMC of the net load of the *star* node is superimposed with the LFC of the connecting branch mn. The two curves intersect at 5, 10 and 15 points from which the notches are also predicted. The Δf of the notches noted in the IA plot is (90 kHz, 60 kHz, 100 kHz), (80 kHz, 50 kHz, 300 kHz) and (50 kHz, 60 kHz, 200 kHz), respectively.

Implications The characteristics of the notches for complex topologies like *star* branches can be successfully analyzed using the LFM technique. It is seen that as N is increased, the IMC becomes very small tending to zero and intersects the LFM at the low y values. This restricts the notches to be near the short-circuit positions.

5.1.3 *Bus* Topology

For *bus* topology (Fig. 1c), the number of *bus* components is increased as 1, 2 and 6 and the notches analyzed. For one number of *bus* components, *bus* 1 is connected to the point m in the path XY and the IA of the branch is given by $Y^1_{IN\text{-}BUS}$. *bus* 1 acts like a simple *star* branch with two branches at the nodes. The parallel combination of *bus* 1 and branch ab forms the load of *bus* 2. For two number of *bus* component, *bus* 2 is connected to the point m in the path XY. The IA of the branch is then $Y^2_{IN\text{-}BUS}$. Likewise, the IA for *bus* 6 is

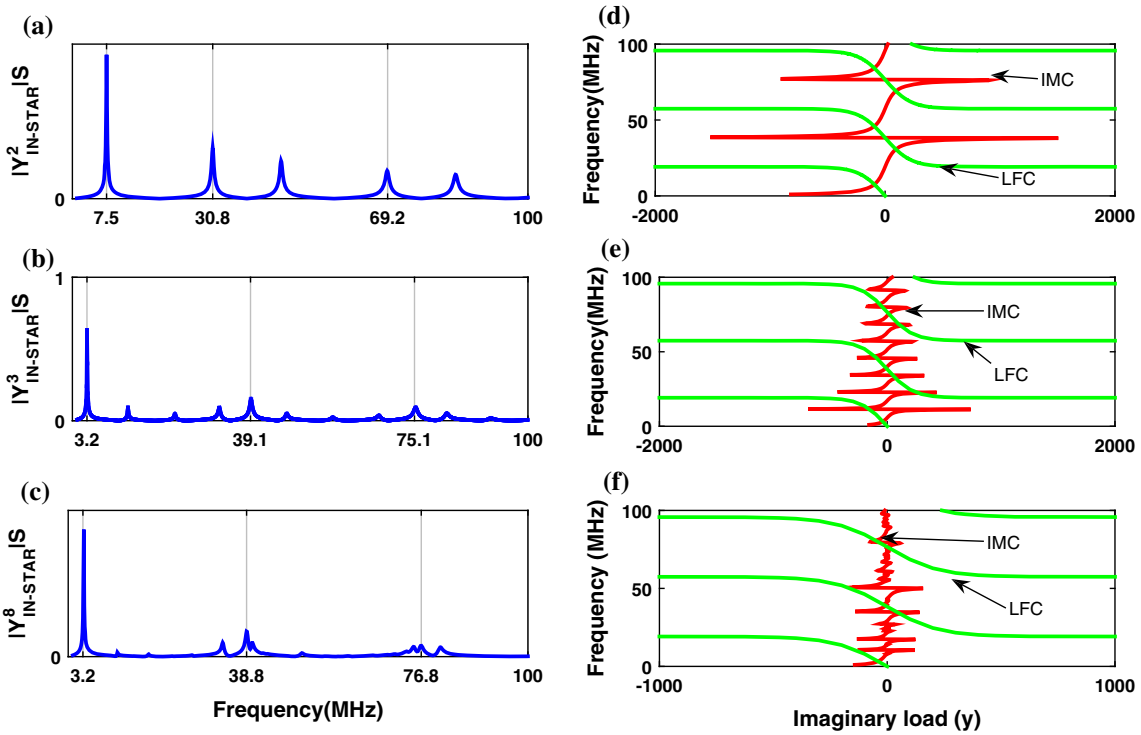

Fig. 7 Verification of the LFM procedure using different a number of branches in *star* topology. The magnitude of the input admittance of the branch in *star* topology in Seimen (S) with **a** 2, **b** 3 and **c** 8 number of branches in the *star* node. The LFM is given in **d**–**f**, respectively

$Y^6_{IN\text{-}BUS}$. In general, the IA of N number of *bus* components or *bus* N connected to m is $Y^N_{IN\text{-}BUS}$ and given by (17) [28].

$$Y^N_{IN\text{-}BUS} = \frac{Y_{N-1} + y_{N-1} + Y_{\text{open\_}N-1}}{1 + Z_0^2\,(Y_{N-1} + y_{N-1})\,Y_{\text{open\_}N-1}} \tag{17}$$

where Y_{N-1} and y_{N-1} are the IA of qp and qn at the node q, respectively, and $Y_{\text{open\_}N-1}$ is the IA of mq if it were open. Figure 8 shows $Y^1_{IN\text{-}BUS}$, $Y^2_{IN\text{-}BUS}$ and $Y^6_{IN\text{-}BUS}$, respectively, with all the branches being open circuits. As seen from the figure, the number of notches increases drastically as the *bus* components are increased. To estimate the notches using the LFM, the IMC of the branch nodes is superimposed on the LFC of the connecting branch and the position of the notches predicted. To find the predicted notches for *bus* 1, the IMC of the impedance at n is superimposed on the LFC of nb. Similarly, to find the predicted notches for *bus* 2, the IMC of the impedance at b consisting of *bus* 1 and ab is superimposed on the LFC of bd and so on. The Δf of the notches marked in the figure are given by (90 kHz, 50 kHz, 100 kHz), (200 kHz, 50 kHz, 250 kHz) and (340 kHz, 50 kHz, 10 kHz), respectively.

Implications: The notches for *bus* branches are also successfully predicted using the LFM technique. As the number of *bus* components is increased, the IMC varies rapidly and intersects the LFM in many points. Thus, the number of notches also increases simultaneously.

5.1.4 Random Simulation of FDLs

The LFM technique is tested in a large ensemble of probable FDLs found in papers. The loads are selected at random (100 numbers in each case) and vary within reported limits, namely capacitors $C \in (0.1, 0.47)_{\text{min,max}}\,\mu$F inductance L $\in (0.1, 100)_{\text{min,max}}$ mH [19,30] and four categories of RLC loads [25]. The four categories are (a) RLC1 having low f_0 and low Q (2 MHz, 5), (b) RLC2 having low f_0 and high Q (2 MHz, 25), (c) RLC3 having high f_0 and low Q (28 MHz, 5) and (d) RLC4 having high f_0 and high Q (28 MHz, 25), respectively. For each of the four categories, R is varied randomly in between 200 and 1800 Ω (Sect. 3.1.3) to make the channels close to reality. The length of the branch is kept constant at $l_{\text{br}} = 2.55$ m. For each of the random channels, the 'actual' and 'predicted' values are found out. The former is found out by evaluating the TF and noting the frequency of the notches. Table 3 gives the mean (μ) and the standard deviation (σ) of the notches in each of the cases. These are represented by (μ_{p}, σ_{p}) and (μ_{a}, σ_{a}), the subscripts denoting the analysis performed using the 'actual' and 'predicted' values. The Δf of each of the randomly generated channels are also estimated and the mean ($\mu_{\Delta f}$) and standard deviation ($\sigma_{\Delta f}$) of the frequency deviation found out. It is seen in the table that $\mu_{\Delta f}$ is as small as 3 kHz and the $\sigma_{\Delta f}$ can be as small as 0.3 kHz. An average error of 100 kHz and average standard deviation of 45 kHz is

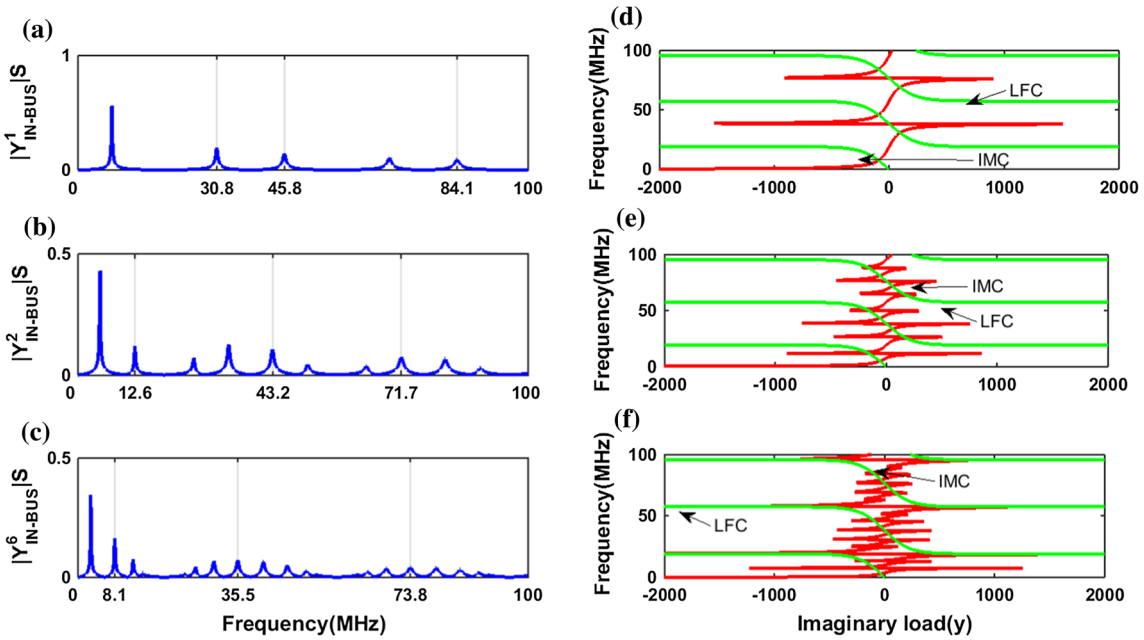

Fig. 8 Verification of the LFM procedure for *bus* topology. The magnitude of the input admittance of the branch in Seimen (S) for *bus* topology with **a** 1, **b** 2 and **c** 6 number of *bus* components. The LFM is given in **d**–**f**, respectively

Table 3 Analysis of the statistical characteristics of the notches using randomly selected capacitive, inductive, resonant RLC loads in a simple branch ($l_{\text{br}} = 2.55$ m) constituted of cable C8

Load types	Notch number	μ_{a} (MHz)	σ_{a} (MHz)	μ_{p} (MHz)	σ_{p} (MHz)	$\mu_{\triangle f}$ (MHz)	$\sigma_{\triangle f}$ (MHz)
Capacitive	1st	0.300	0.1079	0.230	0.055	0.162	0.0500
	2nd	38.37	0.0006	38.29	0.001	0.078	0.0004
	3rd	76.68	0.0003	76.58	0.001	0.103	0.0005
Inductive	1st	19.20	0.0013	19.15	2.80E−14	0.054	0.0013
	2nd	57.53	0.0004	57.44	4.40E−14	0.094	0.0004
RLC1	1st	19.20	0.0013	19.10	0.001	0.100	0.0003
$(f_0, Q) =$	2nd	39.26	0.4042	39.21	0.401	0.003	0.0540
(2 MHz, 5)	3rd	77.13	0.2070	77.05	0.207	0.078	0.0007
RLC2	1st	3.305	0.4911	3.302	0.487	0.011	0.0371
$(f_0, Q) =$	2nd	38.53	0.0850	38.48	0.083	0.047	0.0013
(2 MHz, 25)	3rd	76.76	0.0420	76.68	0.042	0.079	0.0004
RLC3	1st	21.35	2.11	21.90	2.19	0.160	0.0900
$(f_0, Q) =$	2nd	48.72	2.57	48.52	2.20	0.200	0.3200
(28 MHz, 5)	3rd	82.74	2.34	82.94	2.48	0.200	0.1500
RLC4	1st	25.65	0.7140	25.45	0.701	0.201	0.0140
$(f_0, Q) =$	2nd	42.29	1.4100	42.32	1.480	0.070	0.0500
(28 MHz, 25)	3rd	78.13	0.6340	78.06	0.643	0.069	0.0100

obtained, taking into consideration all the notches caused by the loads.

Implications The LFM technique is able to predict the statistical variations in the notches within a limit of error.

5.2 Experimental Test Channels

To validate the LFM method experimentally, four test channels loaded with parallel RLC circuits, namely (i) RLC_1, (ii) RLC_2, (iii) RLC_3, (iv) RLC_1 and RLC_2 are considered. In (i), (ii) and (iii), the branch has a length of $l_{\text{br}} = 2.55$ m, and in (iv), the two loads are placed at two different branches of the same length separately. The TFs are evaluated experimentally, and the magnitude is plotted as shown in Fig. 9a. It is seen that loads (i) and (ii) show notches at 3.4 MHz and 2.4 MHz, respectively, and (iii) does not constitute any. The position of these notches is predicted successfully from the LFM in Fig. 9b up to a maximum error of $\Delta f = 100$ kHz.

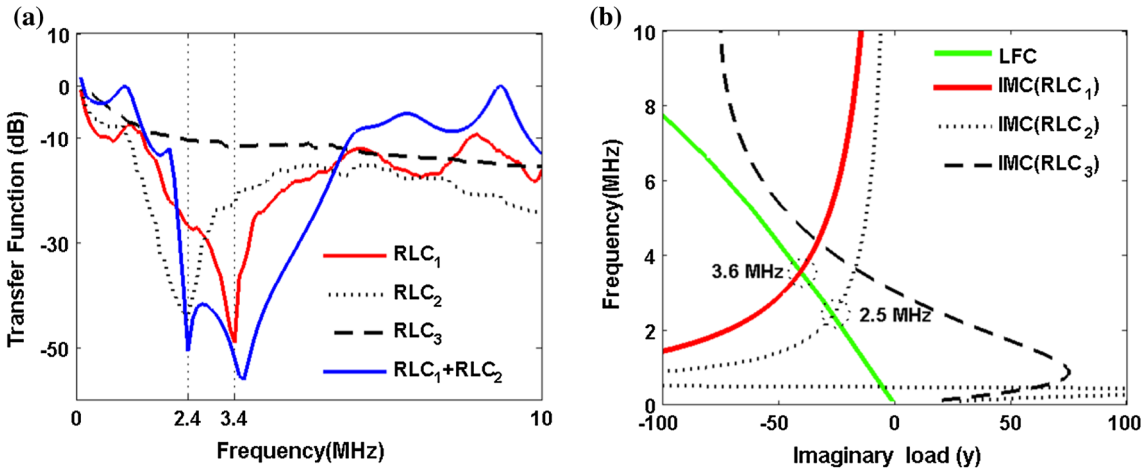

Fig. 9 Verification of the LFM procedure experimentally: **a** magnitude of the transfer function of a power line section with one/two RLC loads obtained practically, **b** LFM for the loads showing the specific LFC and IMCs

Load (iii) does not constitute any notches as the IMC does not intersect the LFC at any frequency. The load (iv) shows two notches at 2.4 MHz and 3.4 MHz

Implications The LFM technique is verified experimentally. The appearance of two notches in (iv) verifies the superposition of resonant nodes and can be predicted by applying the LFM separately for the two branches.

From the simulation and experiments, it is seen that the notches in FDLs or complex topologies can be predicted with considerable amount of accuracy even without evaluating the TF of the channel. The LFM can therefore be considered as an alternate procedure for analyzing the characteristics of the notches for any change in network variables. In the next section, the LFM is used to draw conclusions about the statistical nature of notches as a function loads and the cable parameters.

6 Analysis of the Statistical Characteristics of Notches

In this section, a statistical analysis of the notch variation for random loads in a simple branch is done. The length of the branch is taken to be $l_{\mathrm{br}} = 2.55$ m as before. The analysis is done using all the cables listed in Table 1. The aim is to find out if there is any dependency of the variation in frequency selectivity on the cable parameters due to random loads. The loads used are the random FDLs discussed earlier, namely capacitive, inductive and RLC loads. The RLC loads are grouped into two wide categories: firstly those with lowest f_0 (2 MHz) and secondly those with highest f_0 (28 MHz). The one with lowest f_0 is further divided into RLC1 and RLC2 having low Q (5) and high Q (25) values, respectively. Those with high f_0 are also divided into RLC3 and RLC4 having these Qs, respectively. The number of random channels generated for each type of loads is 100. As before, the values of the random loads are limited by the extreme values reported. For RLC load, only the resistance at resonance R is changed within the given limits, keeping the f_0 and Q fixed in each category. For each load condition, the 'predicted' and 'actual' notch frequencies are evaluated, and the mean and standard deviation of the frequency deviation (necessarily σ_{a} and σ_{p}) for each set of random loads are also found out. This is done for all the cables tabulated in Table 1, and σ_{a} and σ_{p} are plotted verses Z_0. This gives a method of finding the dependency of the statistical nature of the notches on the cable parameters. The results of the analysis are also explained using visual observation of the LFM. The analysis follows three steps: firstly, analysis of the notches for a particular cable namely C26, secondly, analysis of a particular notch for two extreme cable types in Table 1, namely C1 and C26, and thirdly, observing the variation of σ (σ_{a} and σ_{p}) with Z_0 to seek the generalized trends. This is done generating PL channels using all the cables. Similarity of the trends using either methods would conclude the use of the LFM as an alternate method for statistical analysis. The cables C1 and C26 have Z_0 of 268.3 Ω and 7.2 Ω, respectively, and give the cases of minimum and maximum *roll-off* constant w (0.00177 to 0.0655). Thus, the aim is to find the dependency of the statistics of the notches on Z_0 and also to check whether the trends are explainable by the LFM procedure. This would give an alternate method of analysis of notches statistically.

6.1 Analysis of Notches for Capacitive Loads

Figure 10 shows the analysis for randomly selected capacitive loads. Figure 10a shows the LFM for the cable C26 together with the LFC and IMCs. The spread of the intersection frequencies of the IMC and the LFC predicts more

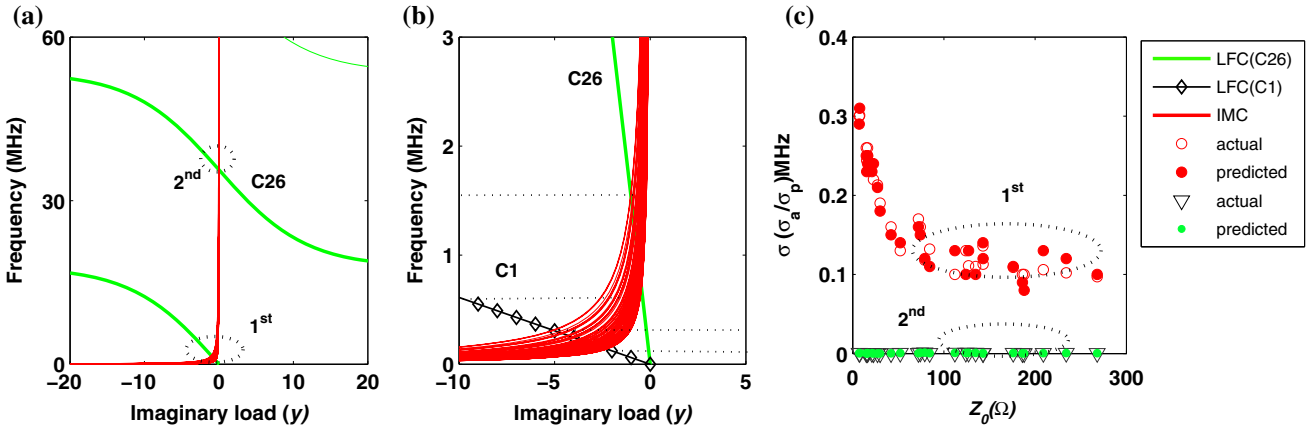

Fig. 10 Analysis of the notches for random capacitive loads: **a** LFM for the cable C26 showing the variations in the first and second notches, **b** LFM for cables C1 and C26 showing the variation in the first notch. The dotted lines show the range of variation for the two cables. **c** Dependence of standard deviation (σ) of the first and second notches on the characteristics impedance of the cables. This is shown for both the 'actual' and 'predicted values (σ_a/σ_p)

variation in the first notch than in the second. Figure 10b shows the LFM of the first notch for both the cables C1 and C26. The IMC profile shows that the predicted values for C26 vary within a larger range than C1. The larger w of C26 has caused the LFC to *roll off* faster and as such the IMC to intersect in a much wider range of frequencies. The reverse is the case for C1. The variations in the intersected curves are shown by the dotted lines in the figure. Using the predicted notches, the standard deviation σ_p is found out. For each channel, the notches are also estimated using the TF and the standard deviation σ_a estimated. This is done for each cable noted in Table 1. Figure 10c shows the plot of σ_p and σ_a with respect to Z_0 of the cables. As expected, both the σ's clearly decrease with the increase of Z_0 which is due to the decrease in w or slower *roll-off* of the LFC The variation in the second notches is much smaller than in the first as expected.

Implications For capacitive loads, the first notch is more prone to variations than the higher-order notches. The higher-order notches are mostly in the short-circuit positions. The notches in the higher Z_0 cables show less variation than in the lower ones.

6.2 Analysis of Notches for Inductive Loads

The analysis for inductive loads is given in Fig. 11. Figure 11a shows the LFM for C26 and Fig. 11b for C1 and C26 for the first notch. It is seen that the notches are always predicted at the open-circuit positions, and as such, the value of σ_p is very small. From a plot of σ_p verses Z_0 in Fig. 11c, it is seen that the same is of the order of 10^{-3} MHz for all the cables. The dependence on Z_0 is random in nature for all the cables and as such cannot be generalized. Similar results are seen in σ_a using the analysis of TF.

Implications For inductive loads, the notches for all the cables are mostly at the open-circuit positions and do not vary much when the values of the loads are changed.

6.3 Analysis of Notches for RLC Loads Having Low Resonant Frequencies

Figure 12 shows the analysis for low f_0 cases in RLC loads. Figure 12a shows the LFM for RLC1 in cable C26. Figure 12b gives a closer look of the first notch for both RLC1 and RLC2 in C1 and C26. It is seen that the spread of IMC for RLC1 is greater than RLC2 for both the cables. This is due to the smaller value of Q for RLC1 compared to RLC2. For both the loads, the spread in C26 is more than C1. This is due to larger values of w in the former. These results are also portrayed from the plot of σ in Fig. 12c. Cables with larger Z_0 or smaller w cause the notches to vary within smaller ranges. Additionally, loads having a wider range of the IMC cause the notches to vary within larger ranges than the otherwise. This causes the value of σ to be greater for RLC1 than RLC2.

Implications For RLC loads having low resonant frequencies, the notches in cables with larger Z_0 are less prone to variations than that with smaller Z_0. Loads with smaller Q lead to larger variation in frequency selectivity compared to larger ones.

6.4 Analysis of Notches for Resonant RLC Loads Having High Resonant Frequencies

Figure 13 shows the analysis for high f_0 cases (RLC3 and RLC4). Figure 13a shows the LFM for RLC3 in cable C26. Here, the second notch caused by the capacitive reactance of the load is considered for analysis. It is seen that though the

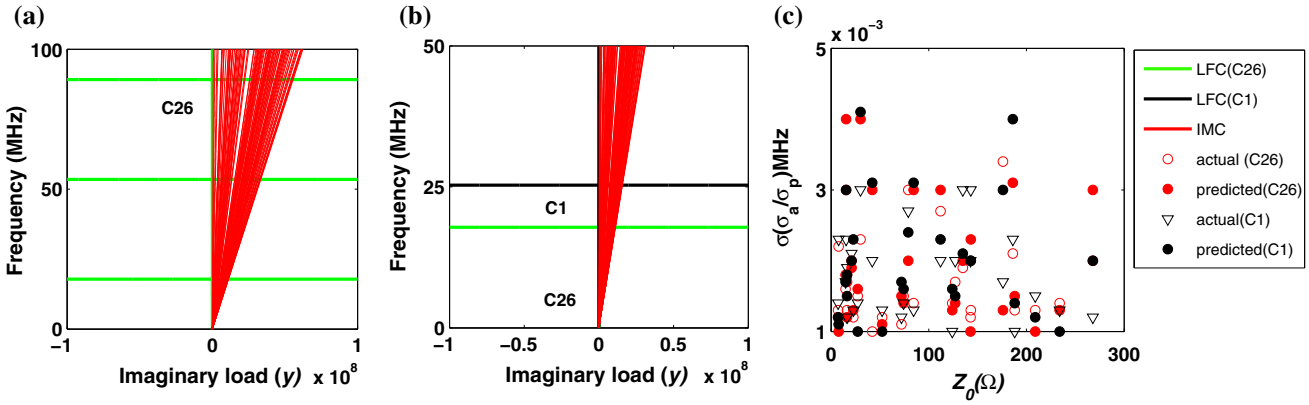

Fig. 11 Analysis of the notches for random inductive loads: **a** LFM for the cable C26. **b** LFM for cables C1 and C26 showing the constant nature of the first predicted notch positions. **c** Plot of the standard deviation (σ) of the first and second notch with respect to the characteristics impedance of the cables. The variation is shown for both the 'actual' and 'predicted' values (σ_a/σ_p)

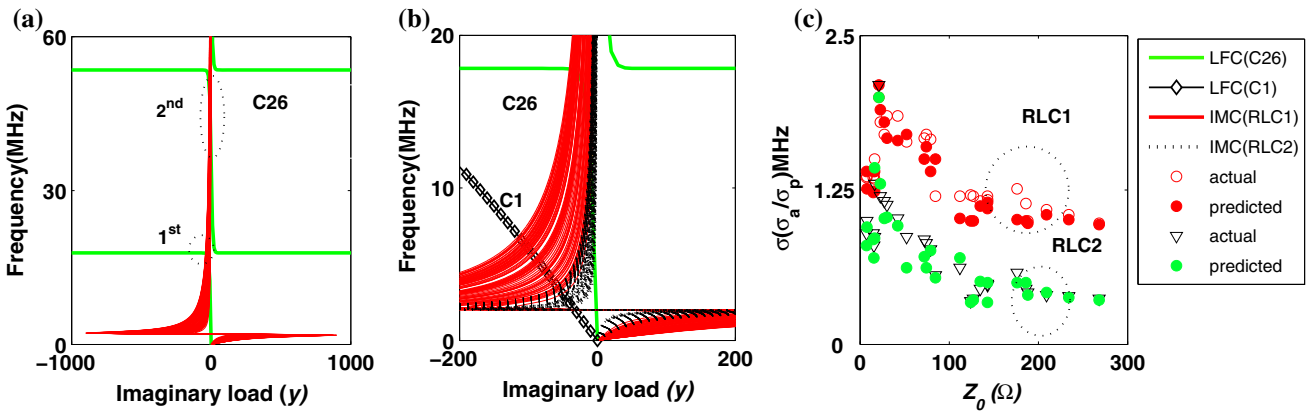

Fig. 12 Analysis of notches for random RLC loads for low f_0 cases: **a** LFM for RLC1 for C26. **b** LFM for RLC1 and RLC2 in C1 and C26 showing the variation in the 'predicted' notch positions. **c** Dependence of standard deviation (σ) of the first notch due to RLC1 and RLC2 on the characteristics impedance of the cables. The variation is shown for both the 'actual' and 'predicted' (σ_a/σ_p)

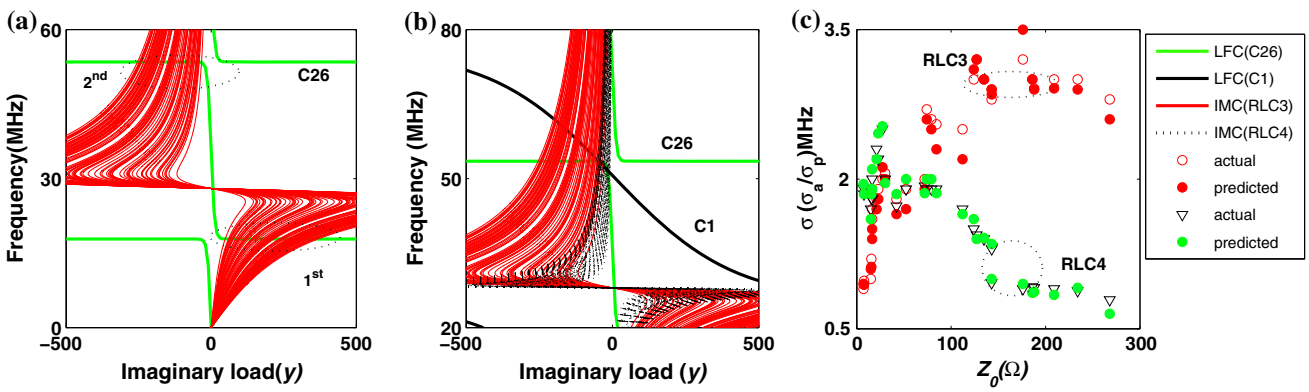

Fig. 13 Analysis of notches for random RLC loads for high f_0 cases: **a** LFM for RLC3 for C26. **b** LFM for RLC3 and RLC4 loads in C1 and C26. **c** Dependence of standard deviation (σ) of the notch due to RLC3 and RLC4 on the characteristics impedance of the cables. The variation is shown for both the 'actual' and 'predicted' (σ_a/σ_p)

spread of the IMC is large, the frequency of intersection with the LFC is mostly in the open-circuit position, causing small deviation of the notches from the mean positions. Figure 13b shows the LFM for both the loads in cables C1 and C26. It is seen that for the cable C26, the spread of the point of intersection of the IMC and LFC is more for RLC4 than for RLC3. This causes the σ to be greater for RLC4 than for RLC3 for low Z_0 cables in Fig. 13c. In C1, for both the loads, the frequency of intersection is in the region that causes a maximum shift from the open- and short-circuit positions. However, as the spread in RLC3 is greater than in RLC4, the σ of the predicted notches is greater for RLC3 than for RLC4 for high Z_0 cables.

Implications For RLC loads having high resonant frequencies, the dependency of the variation in notches for different cables cannot be generalized.

Observing the graphs from Figs. 10c, 11c, 12c and 13c, it is seen that in all the cases, the trend in the statistical nature evaluated using the LFM is similar to that using the TF. As such, the LFM can enable to study the statistical analysis of notches for random loads. The observation of the LFM can also enable the analysis of notches.

7 Results and Discussion

The LFM technique presented has many important contributions in regard to notch prediction and analysis in indoor PL channels.

7.1 Method is Effective for Notch Prediction and Analysis with 4 Parameters Only

The LFM method is effective for notches prediction and analysis for any change in variability. Firstly, the technique requires a maximum of only 4 parameters, namely the length of the branch, the cable parameters (L and C) and the IMC of the loads for effective prediction for any time-invariant FDLs. This is an advantage over the frequency domain bottom-up method because here the notches are determined only after the evaluation of the TF. Secondly, other deterministic methods are successful in predicting only for open- and short-circuit conditions (Sect. 3.2.8). However, for FDLs, the notch can be anywhere between f_k^{open} and f_k^{short}, and the maximum uncertainty or error will be when the notch is in the middle of the two frequencies. For example for the cable C8, the maximum uncertainty will be $(f_k^{\text{open}} \sim f_k^{\text{short}})/2$, i.e., 19.2/2 MHz = 9.6 MHz. Table 4 gives the average error and standard deviation of the error of all the notches analyzed for all the load conditions (except inductive loads) using the LFM technique. As seen from the table, the maximum mean error for C8 is found to be 0.228 MHz, and as such, the maximum error or uncertainty is reduced by $(f_k^{\text{open}} - f_k^{\text{short}})/2 - \mu_{\Delta f}$ or by 97.61% of the earlier value. The table shows a decrease in the prediction error by (99.46–93.63%) considering all the cables. For any change of parameters, the nature of notches can also be estimated by simple analysis of the graphs. Thirdly, the technique is also applicable for analyzing notches due to complex topologies like *star* and *bus* branches in the communication path. The *star* branches lead to lesser frequency-selective channels than *bus* ones as the number of components is increased. Till date, no such prediction or analysis mechanism is available in papers. Table 2 compares the advantage of this method with the other models observed earlier. As seen from the table, the method overcomes most of the limitations encountered. This method is capable of notch prediction within an error; it is able to relate dependency on cable parameters and loads; and also it is able to perform statistical analysis by visual observation without evaluation of the TF.

From Table 4, it is also seen that the error of prediction becomes more as Z_0 is decreased. This is because the appropriate fitting of the locus of the notches with the LFC also decreases as seen by a decrease in the R^2 values (Table 1). As Z_0 decreases, the change in the notch positions for small values of y is very fast and the *roll-off* constant w does not fit these regions effectively. As the LFC is the tool for the mapping procedure, an error in the curves leads to error in the prediction. Another reason for the error is the way the open- and short-circuit notches using (7) and (8) are obtained. In the evaluation of these frequencies, the phase constant of the TL line is taken to be dependent only on L and C. Practically this is not so as the parameter also depends on the other line parameters like the resistance per unit length and the conductance per unit length and these equations are just approximations for high frequencies [28]. The error in prediction can thus be decreased by proper fitting mechanism where these dependencies are also taken into account.

7.2 Statistical Analysis of Notches in Random Channels is Possible Using Simple Means

Using the LFM technique, statistical analysis of the notches is also possible by analyzing the characteristics of the LFC and the IMC. This greatly simplifies the problem, because otherwise there is no way to perform such an analysis till date. Analyzing a large number of random channels, it is found that PL channels are not as unpredictable as thought of, but offer considerable amount of deterministic characteristics even in the large number of variabilities present. Some of the generalizations are: varying the capacitive loads has more effect on the low-frequency notches than the higher ones; the standard deviation for cables with higher Z_0 is lower than that of smaller Z_0; for RLC loads, the variation in the notches is more in the region of the resonant frequency; those having low f_0 and high Q in high Z_0 cables offer minimum variation in the notches; and those with high f_0 and low Q in high Z_0

Table 4 Mean and standard deviation of the frequency deviation of all the cables for the notches analyzed and the improvement in prediction error

Cable [References]	Range between open circuit and short circuit (MHz)	$\mu_{\Delta f}$ (MHz)	$\sigma\Delta f$ (MHz)	Improvement in Prediction error (%)
C1 [17]	24.4	0.065	0.029	99.46
C2 [17]	23.9	0.082	0.044	99.31
C3 [17]	23.5	0.079	0.079	99.32
C4 [18]	3.12	0.041	0.102	97.37
C5 [17]	22.2	0.138	0.088	98.75
C6 [19]	26.2	0.189	0.124	98.55
C7 [17]	20.7	0.204	0.109	98.02
C8 [20]	19.1	0.228	0.123	97.61
C9 [16]	19.2	0.187	0.073	98.04
C10 [19]	23.9	0.173	0.065	98.55
C11 [21]	11	0.193	0.083	96.47
C12 [51]	18.8	0.241	0.195	97.43
C13 [19]	16.1	0.195	0.099	97.58
C14 [19]	23.4	0.292	0.292	97.5
C15 [22]	23.6	0.294	0.294	97.5
C16 [23]	16.7	0.264	0.264	96.83
C17 [23]	17.2	0.387	0.387	95.5
C18 [23]	19	0.355	0.355	96.26
C19 [23]	18.4	0.435	0.435	95.26
C20 [23]	18.8	0.46	0.46	95.1
C21 [24]	39.2	0.496	0.496	97.46
C22 [23]	19.2	0.484	0.484	94.96
C23 [23]	17	0.431	0.431	94.94
C24 [23]	17.8	0.444	0.444	95
C25 [23]	19.4	0.492	0.492	94.92
C26 [23]	17.8	0.567	0.567	93.63

cables cause maximum variations; and inductive loads cause least variations in frequency selectivity. Analysis shows that certain loads, cables and frequency bands yield constant frequency-selective channels and will not affect in insertion of newer loads provided the length of the branch is fixed. In general, the cables with high Z_0 show smaller variations than the lower ones (except for RLC3). As the notches are directly related to the peaks in the impulse response (IR) of the channel [21], a greater variation implies larger variations in the IR. This directly affects the group delay of the channel and becomes very large at these frequencies. As a result of large variations, complex schemes might be necessary for mitigation if the communication BW falls in this region.

8 Conclusion

In this paper, we have addressed the problem of predicting frequency of the notches in indoor PL channel applicable in networks, typical to HAN settings and also extracting generalized features in a myriad of channel variables. A method is presented that enables notches to be predicted within an error limit that is much lesser than the deterministic methods available. The method enables notch prediction without evaluating the actual TF and suffices to have knowledge of only 4 parameters for successful prediction. If the input impedance of any network section is known, then the effect on the frequency selectivity when connected to any branch can also be estimated. Using this method, the statistical nature of notch characteristics for random loads can also be ascertained. The method, however, does not give an idea of the depths and breadths of the notches. However, in practical cases, the notches are characterized by a width that can be compensated by the error range of the predicted notch. This work, therefore, enables a predictive solution of the notch dependencies and completes the effort made by experimental methods and theoretical simulations. The properties analyzed show similar trends when the notches are evaluated using the actual TF. Knowledge of the frequency selectivity will give an idea of the average channel gain, having a negative correlation with

the RMS-DS. These parameters have a direct impact on the choice of important system parameters [47]. The results of the paper can be used to get a clearer understanding of the PL channel and aid future designs of cables and modeling of loads. Such a study will enhance the power grid for value-added services used exclusively or as components of hybrid networking infrastructure.

References

1. Kashef, M.; Torky, A; Abdallah, M.; Al-Dhahir, N.; Qaraqe, K.: On the achievable rate of a hybrid PLC/VLC/RF communication system. In: IEEE Global Communications Conference, GLOBECOM 2015 (2015). https://doi.org/10.1109/GLOCOM.2015.7417378
2. Chatterjee, S.; Baishya, R.; Khan, K.; Sarma, P.; Tiru, B.: Characteristics of visible light communication using light-emitting diodes. In: Proceedings of the International Conference on Computing and Communication Systems, pp. 505–513 (2018)
3. Tiru, B.: Exploiting power line for communication purpose: features and prospects of power line communication. In: Sarma, K., Sarma, M., Sarma, M. (eds.) Intelligent Applications for Heterogeneous System Modeling and Design, pp. 320–334. IGI Global, Pennsylvania (2015)
4. Biglieri, E.: Coding and modulation for a horrible channel. IEEE Commun. Mag. **41**, 92–98 (2003)
5. Tiru, B.; Boruah, P.K.: Multipath effects and adaptive transmission in presence of indoor power line background noise. Int. J. Commun. Syst. **23**(1), 63–76 (2010)
6. Baishya, R.; Tiru, B.; Chatterjee, S.; Sarma, U.; Gogoi, K.: Time dependent indoor power line background noise: analysis, simulation and effect on communication system: study of indoor power line noise environment. In: Proceedings International Conference on Advances in Electrical, Electronic and Systems Engineering (ICAEES), pp. 621–625. IEEE (2016)
7. Zhu, W.; Zhu, X.; Lim, E.; Huang, Y.: State-of-art power line communications channel modelling. Procedia Comput. Sci. **17**, 563–570 (2013)
8. Tlich, M.; Zeddam, A.; Moulin, F.; Gauthier, F.: Indoor power-line communications channel characterization up to 100 MHz-part II: time–frequency analysis. IEEE Trans. Power Deliv. **23**, 1402–1409 (2008)
9. Tiru, B.; Boruah, P.K.; Medhi, H.: A DSP based channel selection algorithm for adaptive transmission in indoor power line. Indian J. Phys. **84**(6), 745–749 (2010)
10. Tiru, B.; Boruah, P.K.: Design and testing of a suitable transceiver for full duplex communication in indoor power line. IETE J. Res. **56**(5), 286–292 (2010)
11. Tiru, B.: A novel method of computation of transfer function of unknown networks for indoor power line communication: transfer function estimation of power line using transmission matrices. In: Proceedings of IEEE Symposium on Computational Intelligence for Communication Systems and Networks (CIComms). IEEE (2014)
12. Galli, S.; Banwell, T.C.: A deterministic frequency-domain model for the indoor power line transfer function. IEEE J. Sel. Areas Commun. **24**, 1304–1316 (2006)
13. Galli, S.; Banwell, T.: A novel approach to the modeling of the indoor power line channel-part II: transfer function and its properties. IEEE Trans. Power Deliv. **20**, 1869–1878 (2005)
14. Tonello, A.M.: Wideband impulse modulation and receiver algorithms for multiuser power line communications. EURASIP J. Adv. Signal Process. **1**, 096747 (2007)
15. Tonello, A.M.; Versolatto, F.: Bottom-up statistical PLC channel modeling-part II: inferring the statistics. IEEE Trans. Power Deliv. **25**, 2356–2363 (2010)
16. Tsuzuki, S.; Yamamoto, S.; Takamatsu, T.; Yamada, Y.: Measurement of Japanese indoor power-line channel. In: Proceedings of 5th International Symposium on Power-Line Communication and Its Applications (ISPLC), pp. 79–84 (2001)
17. Marrocco, G.; Statovci, D.; Trautmann, S.: A PLC broadband channel simulator for indoor communications. ISPLC 2013—2013 IEEE 17th International Symposium on Power Line Communications and Its Applications, pp. 321–326 (2013). https://doi.org/10.1109/ISPLC.2013.6525871
18. Tan, B.; Thomson, J.: Parameter appendix. http://www.arxiv.org/pdf/1203.3245.pdf. Accessed 4 May 2016
19. Sutterlin, P.; Downey, W.: Power line communication tutorial-challenges and technologies. https://www.coursehero.com/file/16006749/PLApps-Studywos/. Accessed 16 July 2018
20. Tiru, B.: An analysis of frequency selectivity of indoor powerline channel for broadband communication. ARPN J. Eng. Appl. Sci. **13**(6), 2213–2220 (2018)
21. Mlynek, P.; Misurec, J.; Koutny, M.: Random channel generator for indoor power line communication. Meas. Sci. Rev. **13**, 206–213 (2013). https://doi.org/10.2478/msr-2013-0032
22. Montoya, L.: Power line communications performance overview of the physical layer of available protocols. http://wenku.baidu.com/view/a30b221252d380eb62946d64. Accessed 4 May 2015
23. Ahola, J.: Applicability of power-line communications to data transfer of on-line condition monitoring of electrical drives. ISBN 951-764-783-2 (2003)
24. Hossain, E.; Khan, S.; Ali, A.: Modeling low voltage power line as a data communication channel. Int. J. Electr. Comput. Eng. **2**, 1766–1770 (2008)
25. Canete, F.J.; Cortes, J.A.; Diez, L.; Entrambasaguas, J.T.: A channel model proposal for indoor power line communications. IEEE Commun. Mag. **49**, 166–174 (2011)
26. Tonello, A.M.; Tao, Z.: Bottom-up transfer function generator for broadband PLC statistical channel modeling. In: IEEE International Symposium on Power Line Communications and Its Applications. IEEE (2009)
27. Tonello, A.M.; Versolatto, F.: Bottom-up statistical PLC channel modeling—part I: random topology model and efficient transfer function computation. IEEE Trans. Power Deliv. **26**(2), 891–898 (2011)
28. Tiru, B.: Characteristics of transfer function of power lines having tapped branches in the propagation path. In: Proceedings of International Conference on Computing, Communication and Security, ICCCS 2015 (2016). https://doi.org/10.1109/CCCS.2015.7374152
29. Tiru, B.; Baishya, R.; Sarma, U.: An analysis of indoor power line network as a communication medium using ABCD matrices effect of loads on the transfer function of power line. In: Bora, P., Prasanna, S., Sarma, K., Saikia, N. (eds.) Advances in Communication and Computing. Lecture Notes in Electrical Engineering, vol. 347, pp. 171–181. Springer, New Delhi (2015)
30. Anatory, J.; Member, S.; Theethayi, N.; Kissaka, M.M.; Mvungi, N.H.; Thottappillil, R.; Member, S.: The effects of load impedance, line length, and branches in the BPLC—transmission-lines analysis for indoor voltage channel. IEEE Trans. Power Deliv. **22**(4), 2150–2155 (2007)
31. Zwane, F.; Afullo, T.J.O.: An alternative approach in power line communication channel modelling. Prog. Electromagn. Res. C **47**, 85–93 (2014)
32. Rennane, A.; Konaté, C.; Machmoum, M.: A simplified deterministic approach for accurate modeling of the indoor power line channel. In: Proceedings of Third International Conference on Systems and Networks Communications, pp. 121–126 (2008)

33. Berger, L.T.; Schwager, A.; Escudero-Garzás, J.J.: Power line communications for smart grid applications. J. Electr. Comput. Eng. **3**, 1–17 (2013)
34. Report on presenting the architecture of PLC system, the electricity network topologies, the operating modes and the equipment over which PLC access system will be installed. IST Integrated Project No 507667. Funded by EC , December 2005
35. Specification of PLC System Requirements. IST Integrated Project No 507667. Funded by EC , May 2004
36. Tran-Anh, T.; Auriol, P.; Tran-Quoc, T.: Distribution network modeling for power line communication applications. In: Proceedings of International Symposium on Power Line Communications and Its Applications, pp. 361–365. IEEE (2005)
37. Papadopoulos, T.A., et al.: Medium voltage network PLC modeling and signal propagation analysis. In: Proceedings of IEEE International Symposium on Power Line Communications and Its Applications. IEEE (2007)
38. Samimi, M.H.; Ahmadi-Joneidi, I.; Majzoobi, A.; Golshannavaz, S.: Appropriate selection of shunt compensation reactor in parallel transmission lines: a case study. Int. J. Electr. Power Energy Syst. **96**, 163–173 (2018)
39. Figueiredo C.E.C.; Silveira M.S.; Dos Santos G.J.G.; De Jesus N. C.; Quadros L.: Series compensation on medium voltage radial system. In: Proceeding of 23rd International Conference on Electricity Distribution (2015)
40. Cataliotti, A.; Daidone, A.; Tinè, G.: Power line communication in medium voltage systems: characterization of MV cables. IEEE Trans. Power Deliv. **23**(4), 1896–1902 (2008)
41. Abdelaziz, A.Y.; Ali, E.S.; Elazim, S.A.: Flower pollination algorithm and loss sensitivity factors for optimal sizing and placement of capacitors in radial distribution systems. Int. J. Electr. Power Energy Syst. **78**, 207–214 (2016)
42. Ali, E.S.; Elazim, S.A.; Abdelaziz, A.Y.: Improved harmony algorithm and power loss index for optimal locations and sizing of capacitors in radial distribution systems. Int. J. Electr. Power Energy Syst. **80**, 252–263 (2016)
43. Antoniali, M.; Tonello, A.M.: Measurement and characterization of load impedances in home power line grids. IEEE Trans. Instrum. Meas. **63**(3), 548–556 (2014)
44. Corripio, F.J.C.; Arrabal, J.A.C.; Del Río, L.D.; Muñoz, J.T.E.: Analysis of the cyclic short-term variation of indoor power line channels. IEEE J. Sel. Areas Commun. **24**, 1327–1338 (2006). https://doi.org/10.1109/JSAC.2006.874402
45. Tonello, A.M.; Versolatto, F.; Pittolo, A.: In-home power line communication channel: statistical characterization. IEEE Trans. Commun. **62**, 2096–2106 (2014)
46. Tiru, B.; Boruah, P.K.: Modeling power line channel using ABCD matrices for communication purposes. In: Proceedings of International Conference on Future Electrical Power and Energy Systems Lecture Notes in Information Technology, vol. 9, pp. 374–379 (2012)
47. Galli, S.; Corporation, P.; Blvd, S.W.; Jose, S.: A simplified model for the indoor power line channel. In: Proceedings of IEEE International Symposium on Power Line Communications and Its Applications, pp. 13–19 (2009)
48. Tlich, M.; Zeddam, A.; Moulin, F.; Gauthier, F.; Avril, G.: A broadband powerline channel generator. In: IEEE International Symposium on Power Line Communications and Its Applications, ISPLC'07, pp. 505–510 (2007). https://doi.org/10.1109/ISPLC.2007.371176
49. Rasool, B.; Rasool, A.; Khan, I.: Impedance characterization of power line communication networks. Arab. J. Sci. Eng. **39**(8), 6255–6267 (2014)
50. Mosalaosi, M.; Afullo, T.J.O.: A deterministic channel model for multi-access broadband powerline communication. In: IEEE AFRICON Conference 2015, November (2015)
51. Berger, L.T.; Moreno-Rodríguez, G.: Power line communication channel modelling through concatenated IIR-filter elements. J. Commun. **4**, 41–51 (2009)
52. Anatory, J.; Kissaka, M.M.; Mvungi, N.H.: Channel model for broadband power-line communication. IEEE Trans. Power Deliv. **22**, 135–141 (2007)